NTNU

Norwegian University of
Science and Technology

Critical Behaviour of the Local Load Sharing Fiber Bundle Model

Magnus Holter-S Dahle

Master of Science in Physics and Mathematics
Submission date: January 2016
Supervisor: Alex Hansen, IFY

Norwegian University of Science and Technology
Department of Physics

Abstract

A generalised, history independent, Local Load Sharing Fiber Bundle Model, describing damage propagation in materials as failing fibers under under external load is studied. If the fibers' thresholds t are drawn from an exponential probability distribution $p(t)$ with a cut-off parameter t_0, the model exhibits a transition when adjusting this cut-off parameter. The transition results in a change of behaviour in the damage spreading from being similar to the Equal Load Sharing Fiber Bundle Model, to be dominated by invasion percolation. By investigating this transition, it has been shown that it is indeed a critical phase transition, and the critical cut-off parameter has been determined to $t_c = 0.61 \pm 0.02$. The correlation length exponent of the transition was attempted estimated by the use of the Gradient Method, but did not succeed as the gradient in t_0 induced a forced localisation, independent of the critical cut-off. However, by determining an order parameter for the model, its scaling relation to the system size L, and extrapolating it to infinity, the critical exponent $\beta/\nu = 1.5 \pm 0.1$ was calculated.

Sammendrag

En generalisert, historieuavhengig, lokal last-delende fiberbuntmodell, benyttet for å beskrive skadeforplantning i materialer som last-delende, rykende fibre, er studert. Dersom fibrenes terskelverdier trekkes fra en eskponentialfordeling med en avskjæringsparameter t_0, besitter modellen en overgang når avskjæringsparameteren justeres. Overgangen resulterer i en endring av karakteristikken til skadespredningen fra å oppføre seg liknende den lik last-delende fiberbuntmodellen, til å være dominert av invasjonsperkulasjon. Ved å studere denne overgangen er det vist at denne har en kritisk faseovergang, og den kritiske avskjæringsparameteren er bestemt til $t_c = 0.61 \pm 0.02$. Korrelasjonslengdeeksponenten til overgangen ble forsøkt estimert ved bruk av gradientmetoden, men dette lyktes ikke da gradienten i t_0 medførte en tvungen lokalisering av skadeforplantningen, uavhenging fra den kritiske avskjæringsparameteren. Videre har det blitt identifisert en ordens parameter for modellen. Ordensparameterens skaleringsrelasjon til systemstørrelsen L er undersøkt og ekstrapolert til den termodynamiske grensen for å kunne beregne den kritiske eksponenten $\beta/\nu = 1.5 \pm 0.1$.

Preface

The following material is the result of the research related to my Master's Thesis. It is a study of the apparent critical transition occurring the local load sharing fiber bundle model for a particular, critical cut off in the exponential distribution of fiber thresholds. The first chapter outlines the background and motivation behind this work, and also provides a general introduction to the mathematical theory of the Fiber Bundle Models. Also, previous research will be introduced, before defining this project's problems. In the following chapters, applied methods and algorithms are described before results of the simulations are presented and discussed. The final chapter also summarises the problems with their obtained solutions and results before conclusions are drawn and future work is suggested.

Trondheim, 2016-01-24

Magnus Holter-Sørensen Dahle

Acknowledgments

There are a lot of people that deserve credit for aiding me with my Master's Thesis. There is no doubt that without these colleagues, friends and family, the research summarised within the thesis you now hold in your hands would never have been as great as it is now; if it would have been completed at all.

I would first like to thank my supervisor professor Alex Hansen at the Norwegian University of Science and Technology for his eminent guidance, advices and support during the entire length of this project. But also for providing me with challenging and exiting problems, and excellent people to work with. I would also like to thank postdoctoral researcher Santanu Sinha for his aid with helping me understanding and implementing specific algorithms used in this research.

Then, I would express my sincere gratitude to PhD candidates Jonas T. Kjellstadli and Morten Vassvik for their (as far as I've experienced) unlimited patience when dealing with my both relevant and irrelevant, complicated or trivial, but also straight out silly questions regarding this research. Furthermore, I extend my thanks yo MSc. candidates Eivind Bering, Håkon T. Nygård and Jørgen Vågan for their insightful help and invaluable discussions related to the model itself and also issues with code implementation and its optimisation.

I would also like to acknowledge Silje I. Hansen and Frode Strand from the Reakel Service at NTNU for providing me access to one of the Service's computer clusters, which significantly increasing my overall computing power. Many, many thanks are directed to Jens W. Meisingset and Au-Dung Vuong for providing suggestions and feedback on my written thesis before its submission. I would also like to thank my mother, father and brother, for encouraging my pursuit in physics and engineering, and for always expressing genuine interests in what I do.

Finally I thank my dearest Monica Darvik, for her absolute trust, love and care; for her always believing in me, and supporting my work even though it's mostly just Greek to her. Literally. She truly makes me a better Physicist.

MHSD

January, 2016

Contents

Acronyms and Abbreviations

CDF Cumulative Distribution Function

CPU Central Processing Unit

ELS Equal Load Sharing

FBM Fiber Bundle Model

LEFM Linear Elastic Fracture Mechanics

LLS Local Load Sharing

NLEFM Non-Linear Elastic Fracture Mechanics

NTNU Norwegian University of Science and Technology

PDF Probability Distribution Function

Nomenclature

Θ	Order Parameter
β	Order Parameter Exponent
κ	Hookean Spring Constant
ν	Correlation Length Exponent
ξ	Correlation Length
$\mathbb{F}$	Set of all Fibers in the Bundle
$\mathbb{S}$	Set of Surviving Fibers in the Bundle
D_{bf}	Fractal Dimension of the Broken Fracture Front
D_{if}	Fractal Dimension of the Intact Fracture Front
F	External Force/Load on System
L	System Size
N	Total Number of Fibers
S	Percolation Strength
g	Imposed, Spatial Gradient in the Cut-Off Parameter
h	Cluster Size
k	Total Number of Broken Fibers
l_{bf}	Length of the Broken Fracture Front
l_{if}	Length of the Intact Fracture Front
n_c	Total Number of Clusters
p	Perimeter Size

t_0 Cut-Off Parameter in the Fibers' Thresholds' Probability Distribution

t_c Critical Cut-Off Parameter in the Fibers' Thresholds' Probability Distribution

t_j Threshold of the Fiber j

w_f Width of the Complete Fracture Front

x_B Extension of the Fiber Bundle due to the External Force

x_f Position of the Complete Fracture Front

x_j Extension of the Fiber j

$\tilde{w}_f$ Width of the Reduced Fracture Front

$\tilde{x}_f$ Position of the Reduced Fracture Front

List of Figures

1 Introduction

Material fracture, failure modelling and damage propagation are vast topics within multiple fields of applied mathematics, physics and engineering in general [1, 2]. The theory of fracture mechanics has changed significantly since da Vinci performed his experimental fracture tests on iron wires [2]. It was first after the introduction of Griffith's fracture criterion [3], that the material failure became a theoretical research field, and given an extensive mathematical description [2]. Not earlier than 1957, did Irwin developed the concept the energy release rate and applied Westergaard's work [4] to establish the theory of the stress intensity factor [5]. This classical theory of fracture mechanics is commonly referred to as linear elastic fracture mechanics (LEFM), as the the theory is based on the assumption that any external load on a material results in stress within the material which is linearly proportional to the applied external load [6]. For high stresses, the linearity breaks, and the theory of non-linear elastic fracture mechanics (NLEFM) should be applied [6]. When a real medium is exposed to strain, it will cause deformation in the material, which may, or may not be reversible depending on the material and the characteristics of the strain.

The Soft Clamp Fiber Bundle Model treats fracture and encapsulates these deformation effects [6, 7], however it is not history independent. That is, the state of the system depends on what happened earlier in the process, such that it is not necessarily possible to determine how forces are distributed within the system, without knowing its history [1]. From a physicist's point of view, models should be kept simple, to ensure that the fundamental concepts of the physical properties of the modeled system are preserved. An alternative to the Soft Clamp Model is the Local Load Sharing Fiber Bundle Models, which in a simple manner accounts for deformations occurring during fracture, but do so while still being history independent [1].

1.1 The Fiber Bundle Model and Percolation Theory

The Fiber Bundle Model (FBM) was first introduced by Peirce in 1926 to study the weakest link of cotton yarns, by modeling a yarn as a set of Hookean springs referred to

as fibers [8]. Since then, the model has received much attention and later been applied for modelling material fracture and system failures [1, 9, 10]. The model's fundamental principles are essentially quite simple: A finite set $\mathbb{F}$, of N fibers, connects two solids separated by some distance as shown in Figure 1.1. The model then assumes that the fibers behave like Hookean springs, so that if the lower solid is kept stationary while pulling the upper solid up with an external force F to some finite separation x_B, the fibers will be stretched out of their equilibrium position.

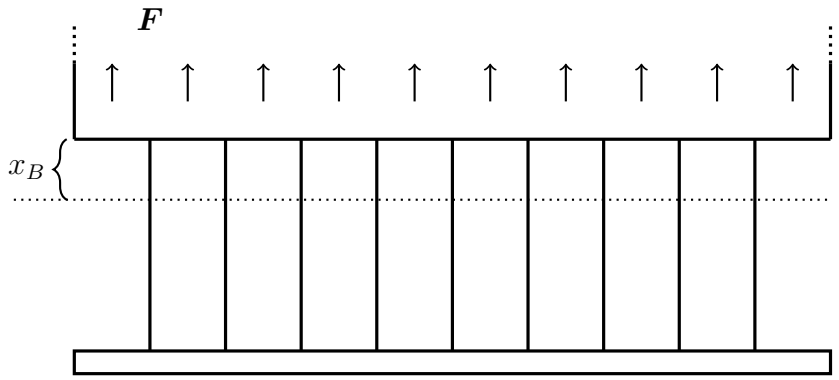

Figure 1.1: The Fiber Bundle Model describes two solids connected by a set (or bundle) of fibers which behaves like Hookean springs. When pulling the system apart by applying an external force F on one of the solids, each fiber i is stretched a distance x_i out of equilibrium which may, or may not, be equal for individual fibers. If no fibers have broken, then $x_i = x_B$ for all i as illustrated. The combined Hookean forces from all intact fibers balances the external force and leave the system in equilibrium, as long as F is held constant.

Moreover, the model introduces an upper threshold (or strength) t_i, drawn from some probability distribution function (PDF) which represents the minimum force a fiber i cannot carry without breaking. The PDF used for this research is mainly the exponential distribution,

$$p(t) = \exp(t_0 - t), \quad t_0 \leq t < \infty, \tag{1.1}$$

where t_0 is the cut-off parameter. One can then study how the system behaves as the increasing external force F pulls the solids apart, overloading fibers beyond their thresholds and breaks the system fiber by fiber. Furthermore, the external force F is assumed to be uniformly distributed over the solid, such that it will be perfectly balanced by the sum of the forces carried by each single fiber. Let $\mathbb{S} \subset \mathbb{F}$ represent the set of surviving fibers. Then, the force on each surviving fiber is proportional by some spring

constant κ_i, to the extension x_i from equilibrium that this particular fiber i experiences, yielding

$$f_i = \begin{cases} \kappa_i x_i, & \forall\, i \in \mathbb{S} \\ 0, & \forall\, i \notin \mathbb{S} \end{cases} . \tag{1.2}$$

The external force must always be balanced by the sum of forces carried by each individual, surviving fiber, implying that forces earlier carried by newly broken fibers must somehow be shared among the remaining fibers. Let k be the number of broken fibers, so that

$$F = \sum_{j \in \mathbb{S}} f_j = \sum_{j=1}^{N-k} \kappa_j x_j \,. \tag{1.3}$$

There are multiple different approaches on how to define the load sharing of surviving fibers, two of them being qualitatively illustrated and summarized in Figure 1.2. For simplicity, assume henceforth that $\kappa_i = \kappa$ for all $i \in \mathbb{F}$. The first load sharing mechanism, as introduced by Peirce [8], is the Equal Load Sharing (ELS) where all surviving fibers equally divide the external force among themselves, resulting in $f_j = F/(N-k)$ for all $j \in \mathbb{S}$ and $f_i = 0$ for all $i \notin \mathbb{S}$. Another sharing mechanism is the Local Load Sharing (LLS), for which the load of broken fibers are distributed among its surviving, nearest neighbours only.

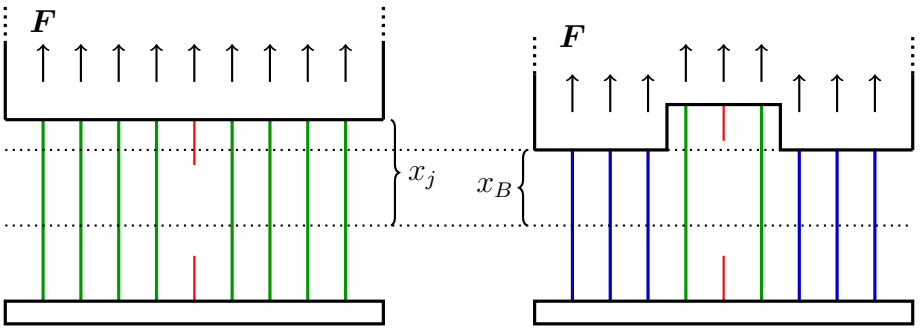

(a) Equal Load Sharing (c) Local Load Sharing

Figure 1.2: The Load Sharing Mechanism of the FBM can be conducted in a number of different ways, two of them qualitatively illustrated in this figure: Red fibers are broken, green fibers are carrying some of the broken fibers' strain and blue fibers are currently unaffected by broken fibers. (a) Applying Equal Load Sharing implies that the strain previously carried by broken fibers are equally distributed among all surviving fibers in the bundle. (b) The Local Load Sharing model makes intact fibers carry the force of their nearest neighbouring broken fibers.

Depending on which definition of load sharing is applied, the model behaves quite differently, and the different approaches of load sharing can be physically interpreted as how soft the modeled material is. In this manner, the ELS describes the two connected plates as infinitely stiff, while the medium (of the upper solid) in the LLS would be soft [1, 6, 7]. In comparison, the Soft Clamp Model could be considered to be somewhere in between the two. This work, however, will only consider the LLS FBM, on a two-dimensional, squared lattice.

Before the LLS FBM is discussed in detail, the reader should get familiar with the fundamentals of percolation theory, which, summarized in one sentence, is the study of clusters [11]. A percolation system consists of nodes, or bonds, that settle in one of multiple possible states, typically just two. A *cluster* is then defined as a set of connected nodes of the same state. Thus, two nodes belong to the same cluster if there exists a connected path of nodes of the same state between them. The nature of connectivity however, depends on the system one studies. If a cluster connects two opposite edges of a finite size system, that is, it spans over one characteristic length of the entire finite system, it is referred to as a *spanning cluster*. When considering the LLS FBM, a fiber always appears in one of two possible states: It is broken or intact, and becomes part of a cluster by connecting to its nearest-neighbours only as illustrated for a two-dimensional system by Figure 1.3. Each broken fiber is assign a cluster label, which defines which cluster of broken fibers it belongs to. From this point on, the term *cluster* will be referring to clusters of *broken* fibers only, if else is not explicitly specified.

1.1.1 The Local Load Sharing Fiber Bundle Model

In one dimension, the fibers of FBM are arranged on a line as shown in Figure 1.1 and one typically applies periodic boundary conditions to reduce finite size effects [1, 12]. For the one-dimensional case, a cluster of broken fibers, regardless of size, will always be bounded by exactly two intact fibers, with the two exceptions of $k = N - 1$ and $k = N$, whereas there is only one or zero intact fibers in the entire bundle, respectively. Thus, an intact fiber in the one-dimensional LLS FBM will experience a load equal to F/N, plus F/N times the the number of broken fibers it neighbours, divided by two: Itself and the other bounding fiber at the other end of the cluster. From this point on, assume $\kappa_i = \kappa$, $\forall i \in \mathbb{F}$, such that with $F = N\kappa x_B$, one has

$$f_j = \frac{\kappa x_B}{N}\left(1 + \frac{h_{j,l} + h_{j,r}}{2}\right). \tag{1.4}$$

Here, $h_{j,l}$ and $h_{j,r}$ are the sizes of the clusters, or holes, immediately to the left and to the right of the surviving fiber j, respectively. Note that this expression is valid, also when $k = N-1$, as long as one applies periodic boundaries. The reader should be careful not to confuse x_B with x_j, as the first is the extension of the fiber bundle as a whole, while the latter is the extension of the individual fiber j. In general, $x_j \geq x_B$ due to deformations in the upper, soft solid, and if no fibers have broken, then $x_j = x_B$ for all j so that $F = \sum_j \kappa x_j = N\kappa x_B$ as depicted in Figure 1.1. Furthermore, it is trivial to generalize equation (1.4) to two, or even higher, dimensions. Again, an intact fiber carries the load of broken neighbours, but for a number of dimensions greater than one, a cluster of broken fibers is no longer bounded by two fibers only. Let the set of intact fibers, which neighbours any fiber of some particular cluster of broken fibers, be the *perimeter* of that cluster. The strain of this cluster is then equally shared among all surviving fibers in this perimeter. All fibers outside the perimeter are unaffected by the broken cluster. Thus, an intact fiber carries the load

$$f_j = \frac{\kappa x}{N}\left(1 + \sum_m \frac{h_{j,m}}{p_{j,m}}\right), \tag{1.5}$$

as it may be part of the multiple perimeters of the multiple, different clusters. Again, h_m gives the size, or number of broken fibers, in cluster m, and p_m represents the number of fibers in this cluster's perimeter. The sum is to be taken over all the different clusters for which the fiber j neighbours, not counting the same cluster more than once. It is trivial to see that (1.4) for the onedimensional model is just a special case of (1.5), as the clusters' perimeters in the one-dimensional case always have size two.

1.1.2 The Process of Breaking Fibers

Consider a system of $N = L \times L$ intact fibers on a squared lattice. Each fiber i is then assigned a threshold t_i representing the minimal load it cannot carry without breaking. Hence, fiber i remains intact as long as $f_i < t_i$, but is referred to as *overloaded* if $f_i \geq t_i$, and will break. If no fibers within the bundle are overloaded, the system is considered to be in an equilibrium state and will not change. This equilibrium is broken by increasing

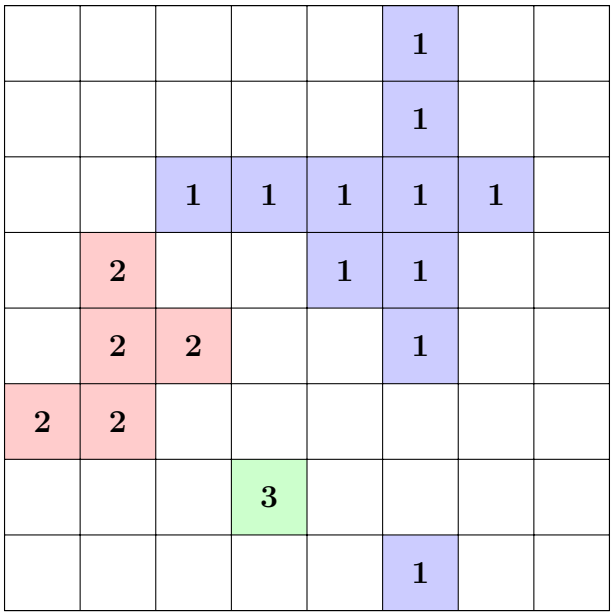

Figure 1.3: The Cluster Label Matrix represents the state of the entire (two-dimensional) $L \times L$ system of fibers. Intact fibers are assigned a predefined label, illustrated by empty (white) cells, while broken fibers are assign the label of the cluster they belong to. Different colors are added to seperate clusters to better distinguish them from each other.

the external force on the system F until the next fiber breaks. Which fiber breaks next is the most heavily loaded[1], currently surviving fiber j found by the *breaking criteria* [1, 10],

$$\max_{j \in \mathbb{S}} \left(\frac{f_j}{t_j} \right) . \tag{1.6}$$

The external force is then raised such that $f_j/t_j = 1$, effectively breaking the fiber j,

$$F = \frac{t_j}{N} \left(1 + \sum_m \frac{h_{j,m}}{p_{j,m}} \right)^{-1} , \tag{1.7}$$

The very first fiber to break will always be the weakest, i.e. the one which was assigned the smallest threshold within the entire bundle, for which the external force will be $F = N \cdot \min_{i \in \mathbb{F}}\{t_i\}$. Immediately after a fiber breaks, the load it carried is divided among its intact neighbours, in accordance with equation (1.5). The system then either reaches a new equilibrium state, or a burst occurs. A *burst* refers to the chain reaction of overloaded fibers due to their newly increased load as a result of neighbouring fibers breaking, without increasing F. The number of fibers breaking in such a burst is referred to as the *burst size* Δ. If $\Delta = N - k$, that is, all currently surviving fibers break, it is said to be a fatal burst resulting in a complete system collapse or failure. Note that during

[1] Relative to its threshold.

a burst, more than one fiber may be overloaded at the same time. This is handled by always breaking the relatively most overloaded fiber determined by the breaking criteria from equation (1.6). Then, the load is redistributed before the breaking criteria is applied again to decide which fiber breaks next. This process is continued until all fibers of the bundle are broken.

1.2 Critical Phenomena and Phase Transitions

The study of critical phenomena and phase transitions is vast and complicated, and only a very brief reveiw will be given here to provide the reader with only the uttermost necessary and fundamental understanding of the theory. For a complete study on critical phenomena and phase transitions, the reader is referred to [12, 13].

A critical phase transition is, rather simplified, a process which significantly changes the behaviour and characteristics of a system when one, or more, parameters of the system are adjusted close to some critical value. A commonly used example is the Ising Model describing how the magnetisation of a system of interacting spins goes from zero to a finite, non-zero quantity when reducing the system's temperature below a critical value. A critical phase transition such as this can described by an order parameter. However, not all phase transitions possesses such an observable quantity. The order parameter defines the transition by being constant, but different, on either side of the transition, effectively representing order and disorder on each side. Typically, the order parameter is zero and non-zero, but finite in these two separated *phases*. Hence, the order parameter is mathematically not an analytical function at the transition point separating the two different regions.

Critical phase transitions are also described by a transition order, typically of first or second order [13]. Second order phase transitions may in general be classified by *critical exponents*, describing the nature of the system's physical properties at, and very close to, the critical transition point [12, 13]. This means that the order parameter's characteristics at the critical transition point can be approximated by power law behaviour. Two such physical properties are to be examined in this research: The order parameter Θ with its order parameter exponent β describing the order and disorder of the system. And the correlation length ξ, with its exponent ν, describing the range of interaction within the

system. If a system exhibits a critical phase transition when adjusting some arbitrary parameter ρ, these physical observables will display power law dependence on their exponent according to

$$\Theta \sim |\rho - \rho_c|^{\beta} \tag{1.8}$$

$$\xi \sim |\rho - \rho_c|^{-\nu}\,, \tag{1.9}$$

where ρ_c is the numerical value of the adjustable parameter ρ at the critical point [12]. These exponents are apparently independent from the details of the system, and are instead characterized by the system's dimension and range of interaction. Hence, obtaining the critical exponents may provide useful insights beyond the limitations of physical system one studies, and also describe behaviour of similar systems. There exists multiple other critical exponents beside β and ν, however, they are all linearly dependent on each other. Hence, determining these two implies obtaining all of them, giving a complete description to this *universality class* of exponents [12, 13].

1.2.1 The Percolation Transition

The reader should be made aware of that percolation systems in general, feature a critical percolation transition when tuning the occupation probability of each individual node in the system, p. An order parameter of this transition is the percolation strength, which is defined as the total number of nodes in the largest cluster of some state, divided by the total number of all nodes settled in this particular state. The percolation strength indicates how the probability for finding a spanning cluster in the system P_s, grows from zero to one as the occupation probability increases beyond its critical value p_c, known as the percolation threshold. The exact critical exponents of this system's universality class are $\beta = 5/36$ and $\nu = 4/3$, for two-dimensional systems [11].

1.2.2 The Localisation Transition

It was discovered that the LLS FBM possesses a localisation transition, for which the damage spreading goes from behaving like the ELS FBM, to be dominated by invasion percolation, when adjusting the cut-off parameter t_0 in the exponential PDF from which the fiber thresholds of the fibers are drawn [10, 14]. To the author's best knowledge, no

other research has yet made attempts to investigate and classify this behaviour.

1.3 Problem Formulation

Sinha, Kjellstadli and Hansen gave a extensive generalization of both the ELS and LLS to higher dimensions [10, 14], and showed that the LLS qualitatively approached the ELS when the system's dimensionality went to infinity. Also, if the fibers' thresholds were drawn from an exponential distribution with a cut-off parameter t_0, they found that the LLS experienced a transition from behaving similar to the ELS for low values of $t_0 \approx 0$, while for higher values ($t_0 \sim 1$), the damage spreading became localized and behaved like invasion percolation [10]. The aim of the current study is to investigate this transition and

- Determine whether or not the change in behaviour is a critical phase transition, and/or can be related to the critical percolation threshold.

If the change in damage spreading behaviour is indeed shown to be a critical phase transition it will be attempted to

- Estimate the critical cut-off parameter t_c , for which the transition occurs.

Moreover, if the above investigations succeed, it will be endeavoured to

- Calculate the critical correlation length exponent ν, and the critical order parameter exponent β.

Under the assumption that the change in behaviour *is* a critical phase transition, independent of the percolation transition, a successful estimation of ν and β, given an accurate calculation of t_c, will imply a complete description of the universality class for this transition [13].

2 Theory, Methods and Algorithms

Assuming the change in behaviour of the damage spreading when adjusting t_0 is indeed a critical phase transition, one first has to locate the transition, that is, determining numerically the critical value t_c. To achieve this, two different approaches are applied and their results compared. The first is the Gradient Method, as first introduced for percolation problems by Sapoval, Rosso and Gouyet [15], and later frequently used to study different kinds of critical behaviour [16, 17, 18, 19]. The second approach, is to find and investigate an order parameter of the system, which should abruptly change its characteristics at $t_0 = t_c$ [12, 13]. However, a more detailed and thorough description on how to iterate the Fiber Bundle system will be given first.

2.1 Simulating the Process of Breaking Fibers

The system of fibers is initiated by assigning each fiber a threshold t_i, drawn from the PDF given by equation (1.1). A computer program can numerically obtain exponentially distributed numbers from the inverted the cumulative distribution function (CDF) of the PDF,

$$t = t_0 - \ln(1 - r), \quad 0 \leq r < 1\,, \tag{2.1}$$

where r is a random number drawn from a uniform PDF. When iterating the system a single time step, one has to

- determine which fiber breaks next and break it, increasing F if necessary,
- update clusters labels of broken fibers,
- redistribute the strain.

The breaking criteria from equation (1.6) decides which fiber breaks next. Previous work [7, 10] utilized the Hoshen-Kopelman algorithm for labeling the clusters of broken fibers, which is fast in the sense that the the entire labeling process is completed by

running over the whole system, each fiber, exactly once. However, running the Hoshen-Kopelman algorithm for each broken fiber is unnecessary as the system for the most part will look identical to itself from the last time step. Instead, one can assign a new cluster label to the newly broken fiber, and merge neighbouring clusters with it. This simple approach will be much more efficient as it is only necessary to check the newly broken fiber's four neighbours instead of running over all N fibers of the system.

The merging of clusters however, should be conducted using the same approach as the Hoshen-Kopelman algorithm applies: A cluster label matrix contains one cell for each fiber, holding the cluster label for that particular fiber. An unique, predefined label represents intact fibers, e.g. zero. Now, if a fiber j has been given the label j, that is, a label equal to its own indice, then it's the root of its own cluster. On the other hand, if the fiber j has been given the label $i \neq j$, then it belongs to the same cluster as the fiber i, which may, or may not, be the root of this particular cluster. Henceforth, when merging two clusters it is sufficient to locate the root of one cluster, and assign to it, the indice of the root of the other cluster.

When all clusters of broken fibers have been labeled correctly, a single sweep over the entire system counts the clusters', and their perimeters', sizes, that is h and p respectively. Yet another sweep is conducted to redistribute the strain by applying equation (1.5). This process is then repeated by starting over and determining which fiber breaks next, until all fibers have broken.

2.2 The Gradient Method

Consider an arbitrary statistical system which experiences a critical transition when adjusting some arbitrary parameter. By imposing a gradient in this parameter along one of the spatial axes, such that the parameter takes its critical value some place within the system, one would expect the appearance of an interface or front approximately at the position for which the adjusted parameter is equal to its critical value. This interface should effectively separate the two different phases on each side of the transition.

The Gradient Method is in general used for studying systems which have reached some form of an equilibrium state. However, this is not the case for the Fiber Bundle Model to be considered within this research. As described in section 1.1.2, the FBM breaks fibers

continuously from the first to the last, modelling a dynamic process. Nevertheless, due to the nature of the system, an imposed gradient in the exponential cut-off parameter from the threshold distribution, increasing t_0 from one end of the system to the other, will imply fibers on one side to be considerably[1] weaker than on the opposite side. Ultimately, this results in a directed damage propagation, appearing as a moving fracture front [6, 7]. The properties of this front may change significantly or display critical behaviour when passing over the position x, corresponding to the critical value of the parameter, related by the gradient g. To avoid a discontinuity in the gradient, the periodic boundaries in the direction of the gradient should be omitted.

Consider a fiber bundle of N fibers arranged on squared $L \times L$ grid. Then, impose a constant gradient in t_0 along the x-axis, such that $t_0 = t_{min} < t_c$ on the west side of the system, and $t_0 = t_{max} > t_c$ on the east edge. The critical value t_c is then expected to appear somewhere in between. Since it has already been suggested that $0 < t_c < 1$ [10], $t_{min} = 0$ and $t_{max} = 1$ are chosen. Hence, the fibers' thresholds are drawn from the exponential distribution

$$p(t) = \exp(t_0 - t), \quad t_0 = gx + B, \quad t_0 \leq t < \infty\,, \tag{2.2}$$

The coordinate system of the grid is defined such that each fiber is placed at integer values of $x, y \in [1, L]$, and is also assigned the indice $i = x_i \cdot y_i \in [1, N = L^2]$. This results in $g = x/(L-1)$ and $B = -g$, so that the expression for the cut-off can be rewritten as $t_0 = (x-1)/(L-1)$.

2.3 Locating the Critical Transition Point

There is no approach which guarantees to locate the critical transition, and hence determining the critical cut-off parameter of this system correctly. In fact, there is no guarantee that it will be possible to locate it at all, even if it exists. However, by investigating the evolution of the directed propagation of the appearing fracture front's properties, e.g. its position, width, length and fractal dimension, as well as the system's strain curve, percolation strength, total number of clusters and its inverse, it is suspected that one or more of these will exhibit critical behaviour near the transition point. The fracture front's

[1] Depending on the incline of the gradient.

position can then be extracted from this point in time, measured in terms of the number of broken fibers k. This position will correspond to an effective, critical threshold t_{eff} for this particular system size L, given by the gradient g.

Due to finite size effects, the critical value of t_0 will only be an effective estimate, and it will have to be calculated for multiple different system sizes and extrapolated to the infinite system size at the thermodynamic limit in order to obtain t_c [12, 17, 20]. However, the emerging, propagating fracture front is expected to have a fractal nature [11, 15, 18] and determining its position may not be a trivial task, depending on how one decides to define the front itself.

When considering the FBM as a percolation problem, a fiber is always settled in one of two possible states, that is, either broken or intact. Assuming there exist two infinite clusters, one of broken and one of intact fibers, one may apply several different definitions for the interface (or front) separating these two clusters. The three interfaces studied in this research are,

(1) The set of nearest-neighbour-connected, outermost fibers of the infinite cluster of broken fibers, referred to as the *broken* front.

(2) The set of intact fibers, referred to as the *intact* front, connected by nearest and next-nearest neighbours, but are **also** nearest neighbours of fibers in the infinite broken cluster.

(3) The set of exactly L fibers, consisting of the outermost fiber from each row, of the broken, infinite cluster. This front is referred to as the *reduced* front.

For more detailed descriptions of these definitions, the reader is referred to [15, 18]. Considering percolation theory, these definitions lead to different behaviour of the interface, and the results should be compared to existing theory. For instance should the intact front be expected have a fractal dimension of $D_{if} = 4/3$ when the damage spreading is localized [11, 18]. When investigating the critical percolation threshold, it has been suggested to locate both the intact and broken fronts, and calculate the effective, *complete* front's position as the mean value of the two's as a superposition [18].

The front-finding-algorithm implemented for this work, is described in detail in appendix B, and studies all three interfaces described above, but calculates the fracture

front's position as the mean of the intact and broken fronts as suggested by [18]. The intact and broken fronts are depicted in Figure 2.1.

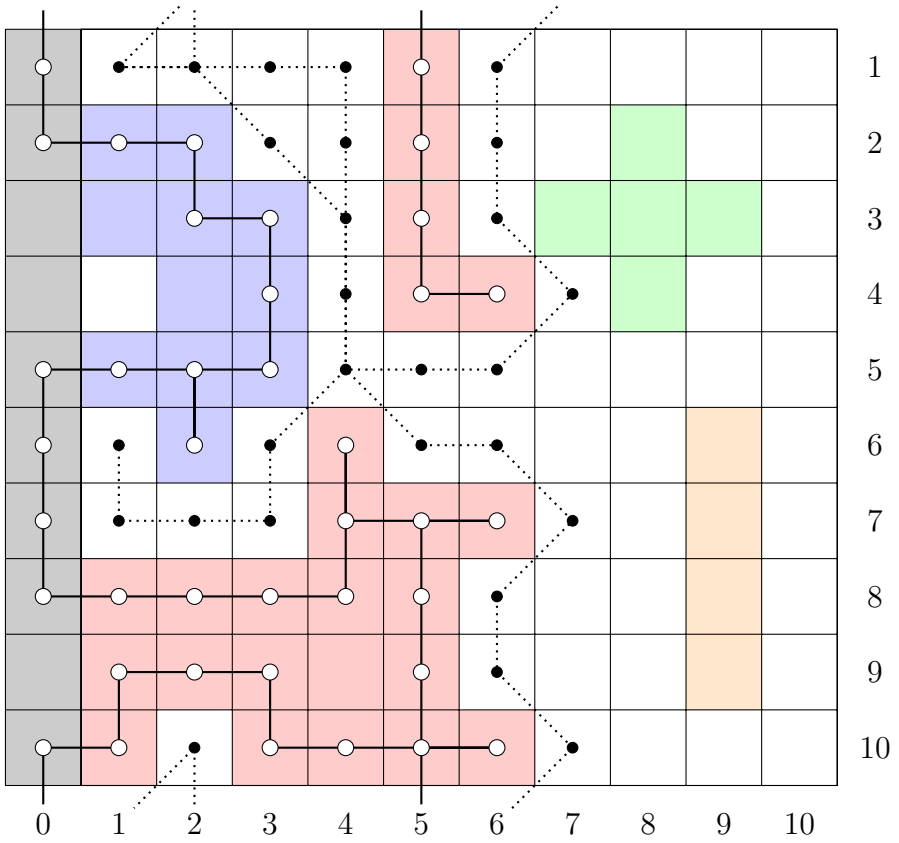

Figure 2.1: The Fracture Front Cluster is defined as the set of clusters which are all connected to the west end of the system, that is, the zeroth column. The position of fracture front is then found by defining it as a super position of the intact and broken fronts as detailed in section 2.3. Cells of different colors belong to different clusters of broken fibers, while white cells represent intact fibers. The solid lines between white dots represent the broken front, while the dotted lines between the black dots represent the intact front. The zeroth column consists of grey cells which are broken ghost fibers.

The complete front's position is calculated by taken the average of the x-coordinate of all partitioning fibers. If there are n_{if} fibers in the intact front, and n_{bf} fibers in the broken front, then

$$x_f = \frac{x_{if} n_{if} + x_{bf} n_{bf}}{n_{if} + n_{bf}} \,. \tag{2.3}$$

Furthermore, $x_{if} = \sum_{i=1}^{n_{if}} x_i$ and equivalently for x_{bf}. The width of the front is simply defined by

$$w_f = \sqrt{\frac{1}{n_{if} + n_{bf}} \sum_{i=1}^{n_{if}+n_{bf}} (x_i - x_f)^2} \,. \tag{2.4}$$

The position $\tilde{x}_f$ and width $\tilde{w}_f$ of the reduced front are defined equivalently to the complete front's. The fractal dimension of any of these fronts is given by

$$D_f = \frac{\log(l)}{\log(L)} \tag{2.5}$$

where l is the front's length, or number of participating fibers. Obviously, the reduced front will always have $D_{rf} = 1$.

2.4 Determining the Correlation Length Exponent

The characteristic length scale of the system ξ, is given from the definition of the correlation length exponent ν

$$\xi \sim |t_0 - t_c|^{-\nu} \,, \tag{2.6}$$

which is only valid when t_0 is very close to its critical value t_c. This correlation length will be equal to the front's width, $\xi = w_f$ at the transition point [15, 17, 18, 20], and one may take advantage of the relation $|t_0 - t_c| = g w_f$ when w_f and t_0 are measured in a region where t_0 is close to t_c. Hence, using the dependence of L in g, one obtains a scaling relation between w and the system size L,

$$\xi = w_f \sim |t_0 - t_c|^{-\nu} \tag{2.7}$$

$$w_f \sim (g w_f)^{-\nu} \tag{2.8}$$

$$w_f \sim g^{-\nu/(1+\nu)} \tag{2.9}$$

$$w_f \sim (L-1)^{\nu/(1+\nu)} \,. \tag{2.10}$$

Thus, Sampling the fronts' width, at the transition point, for multiple, different system sizes enables the estimation of the exponent ν.

2.5 Determining the Order Parameter Exponent

Determining the order parameter exponent β is in general much more difficult than finding ν [12, 17]. An observable system property should first be determined as the system's order parameter Θ. Θ should, in the thermodynamic limit, have the property of being constant everywhere, but in the proximity of the transition. Hence, it is expected to change its constant value during the transition [12]. There is no guarantee that there exists an observable quantity that fits this requirement, however, if one does, it should, according to section 1.2, obey the scaling relation

$$\Theta \sim (t_0 - t_c)^{\beta} . \tag{2.11}$$

For the FBM in consideration, there are at least two possible candidates. (1) The inverted, total number clusters, $1/n_c$. And, (2) the percolation strength S, defined for the FBM as the total number of broken fibers in the largest cluster, divided by the total amount of broken fibers. Both of these quantities will, in the thermodynamic limit as $L \to \infty$, be approximately zero before the transition. Then, increase to unity as the transition occurs and invasion percolation starts dominating the damage spreading process.

Unfortunately, the percolation strength is already a known order parameter for the critical percolation transition as briefly discussed in section 1.2.1. Thus, utilizing S as an order parameter may result in identifying the wrong transition. Hence,

$$\Theta = \left\langle \frac{1}{\max_k\{n_c(k)\}} \right\rangle \tag{2.12}$$

is chosen as the LLS FBM's order parameter. The max value of n_c is used as this point will be well defined in time for any simulation of the process. It should be emphasised that since the FBM simulates a dynamic process, $1/n_c$ will be close to one for the very few first iterations of the system before rapidly decaying.

If one now assumes there exists a critical threshold t_c for which the LLS FBM experiences a critical phase transition. Then, sampling Θ for different t_0, with a given, constant system size L, and examining their dependence should reveal an abrupt, but continuous, change in $\Theta(t_0)$. If $\Theta(t_0)$ is discontinuous at the critical point, the transition is of first

order and not characterised by the power laws with critical exponents [13].

Assuming the transition to be of second order, then for some finite lattice size L, The effective, critical threshold t_{eff} is found by locating the maximum of $\mathrm{d}\Theta/\mathrm{d}t_0$. Due to finite size effects. t_{eff} will deviate from t_c [12, 13, 20]. To obtain t_c, t_{eff} can be extrapolated to the thermodynamic limit by investigating the relation between t_{eff} and the lattice size L, which should the obey scaling relation [12, 20],

$$t_{eff} \sim t_c + A \cdot L^b \,, \tag{2.13}$$

where A and b are unknown constants. Hence, by determining the exponent b which provides the best scaling relation of 2.13, enables the estimation of t_c. If the critical cut-off can be determined with high precision, the critical exponent β/ν may also be determined. At the critical point, the correlation length is, according to (2.6), expected to diverge. For a finite size system, this implies $\xi = L$, if $t_0 = t_c$ in the entire system. By combining equations (2.11) with (2.6) and let $\xi \to L$ by imposing $t_0 = t_c$, one obtains

$$\Theta \sim L^{-\beta/\nu} \,. \tag{2.14}$$

Thus, the order parameter Θ is expected to display power law behaviour with $-\beta/\nu$ as its exponent. The reader should note that the above theory for analysing the order parameter is only valid for systems where the critical parameter $t_0 = t_c$ is kept constant over the entire system. That is, with zero gradient $g = 0$, implying this to analysis to be completely independent of the Gradient Method. The obtained results for t_c should be compared with the corresponding result obtained from the gradient system.

3 Results

All graphs and numerical results presented have been obtained by the author's own implemented computer programs, applying both Fortran and Python code. First to be presented, is the presence of the critical transition itself. Then, the properties of the system and the appearing fracture front is investigated, as the latter develops and propagates through the system in the direction of the gradient. The total number of broken fibers k is applied as a measure of time. Table 3.1 gives an overview of the number of samples used to average system and front properties for different simulations.

L	# of samples per L for gradient system	# of samples per t_0 for $\Theta(t_0)$	# of samples per L for $\Theta(L)$
30	700000	50000	200000
50	300000	30000	100000
75	300000		
100	120000	10000	50000
150	60000		
200	80000		
300	10000	500	4000
500	3470	100	1000
1000	410		

Table 3.1: A summary of the number of samples, which are used to average system and front properties for different simulations.

3.1 The Gradient System

3.1.1 System Evolution and Transition

The apparent phase transition was discovered by comparing the damage spreading of two similar FBM LLS systems, differing only by the cut-off parameter t_0 in their exponential PDF, from which the fiber thresholds were drawn. This result [10] is reproduced and illustrated in Figure 3.1.

When applying the gradient method, as discussed in section 2.2, the system is expected to feature a directed damage propagation, since the fiber strengths will increase along the gradient. Two fiber bundle states from the same simulation, but from two different time-

steps, are shown in Figure 3.2. The emerging fracture interface is highlighted by color in accordance to the fronts' definitions from section 2.3.

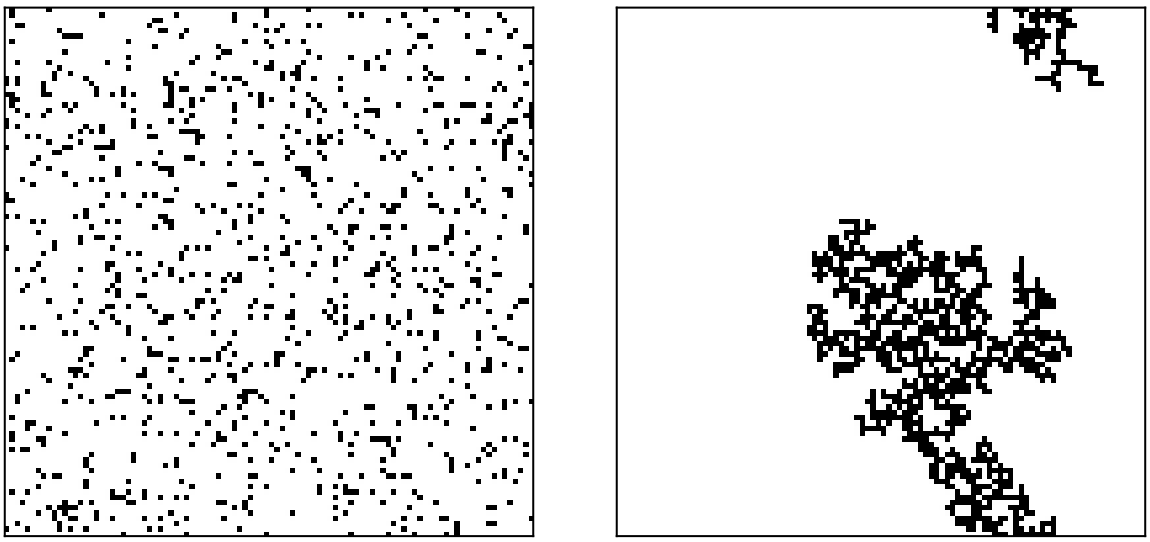

(a) $t_0 = 0.0$. **(b)** $t_0 = 2.0$.

Figure 3.1: The damage spreading of the LLS FBM with constant t_0 behaves significantly different when changing t_0. White cells represents intact fibers and black cells broken fibers. The illustrated systems are both of size $N = 100^2$, and have $k = 1000$ broken fibers.

3.1.2 Fiber Bundle and Fracture Front Properties

The fiber bundle's properties of percolation strength, (inverted) total number of clusters and strain curve as they develop in time k are shown in Figure 3.3 for a system of size $N = 200^2$. The fracture interface is described by the following fronts: The complete front with position x_f and width w_f, and the reduced fronts with position $\tilde{x}_f$ and width $\tilde{w}_f$. The complete front is a super position of the intact, and the broken front, as defined in section 2.3. Their properties are depicted in Figure 3.4, as the develop in time for a $N = 200^2$ system. For the finite size analysis, the properties for various system sizes are presented in Figure 3.8.

3.1.3 The Critical Cut-Off Threshold in the Gradient-System

An effective, critical cut-off threshold t_{eff} is extracted from the local minimum occurring in the complete front's width curve (Figure 3.7a), and plotted against the system size L in

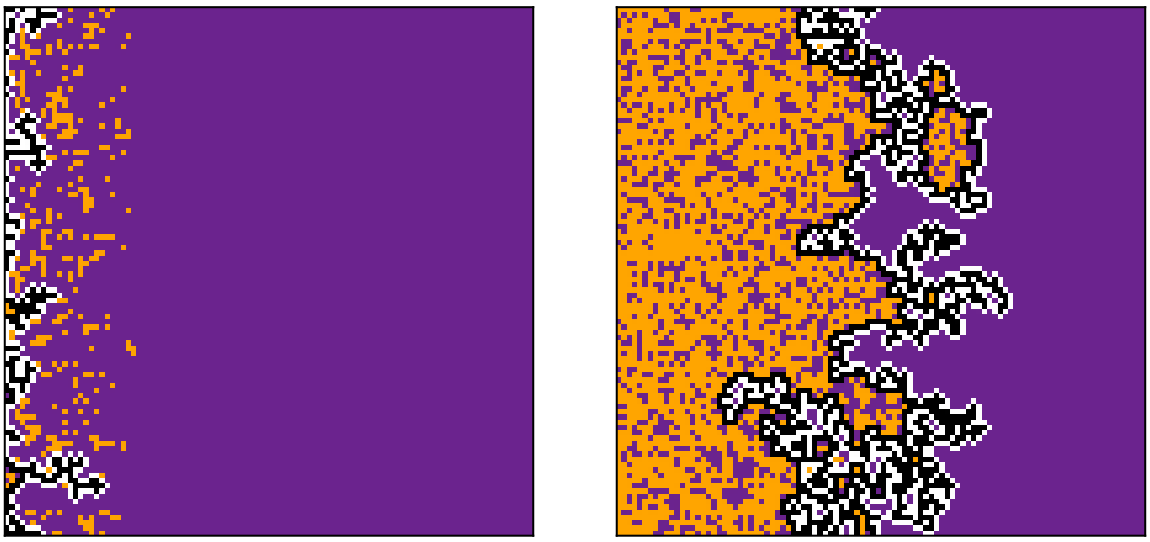

(a) $k = 500$.

(b) $k = 4000$.

Figure 3.2: The damage spreading in the LLS FBM with a gradient in t_0 changes behaviour over time, k. Purple cells represent intact fibers and orange cells broken fibers, while black and white cells represent broken and intact front fibers, respectively, in accordance with the front definitions in section 2.3. If compared with Figure 2.1, note that this illustration does not include the ghost fibers. The illustrated system has $N = 100^2$ fibers, and the gradient linearly increases t_0 from zero on the west end to one on the east end.

search of a power law dependence. However, only $L = \{200, 300, 1000\}$ has been utilized, as the local minimum appears only for $L \geq 150$, and $L = \{150, 500\}$ provided too much noise, preventing a decent power law fit. The obtained value for the critical cut-off was calculated by extrapolating t_{eff} to the thermodynamic limit (Figure 3.11), resulting in $t_c \approx 0.45 \pm 0.1$. The obtained numerical value should be compared with the corresponding value estimate by the analysis of the order parameter. Also, the difficulty of making a decent power law fit should be discussed. The analysis of the complete fracture front's width w_f at the transition point is shown in Figure 3.10 and yielded $\nu \approx 0.57 \pm 0.02$.

3.2 Constant Cut-Off System

When investigating the order parameter described in section 2.5, a system of zero gradient is considered, that is, t_0 is constant throughout the entire system. Then, Θ is sampled for multiple values of t_0 ranging from zero to two, and this is repeated for multiple system sizes. The resulting dependence of the order parameter on t_0, for two different system

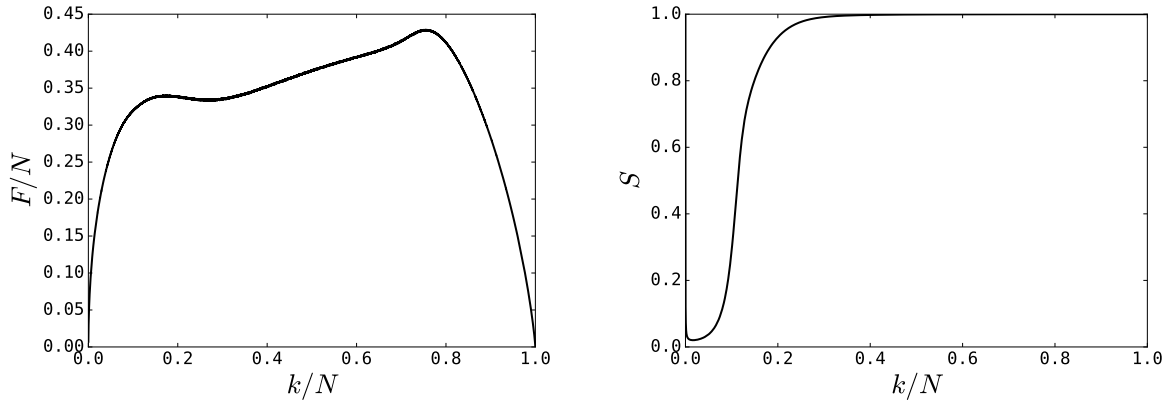

(a) Strain Curve, F/N.

(b) Percolation strength, S.

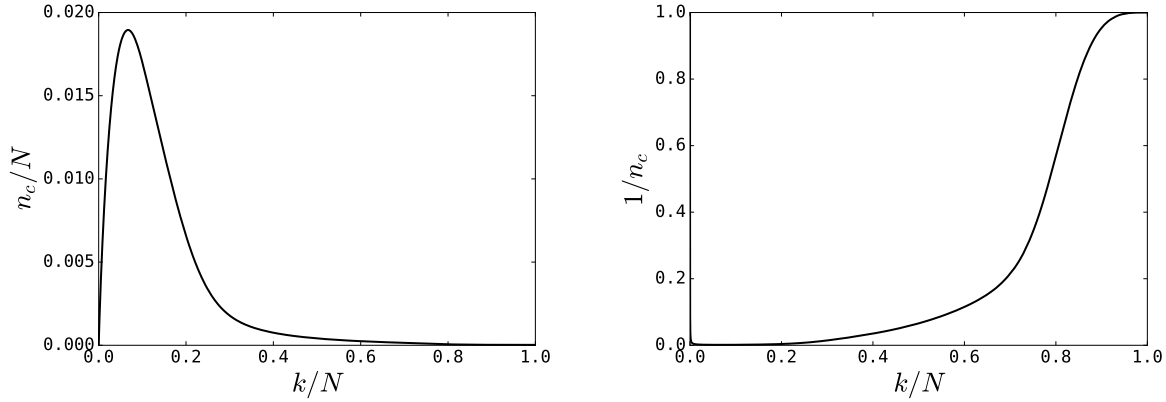

(c) Number of clusters, n_c.

(d) Inverted number of clusters, n_c^{-1}.

Figure 3.3: The resulting system properties for an $N = 200^2$ system. The number of averaging samples for each data point is given by Table 3.1.

sizes, is shown in Figure 3.12, and extrapolated to infinity by a power law fit, illustrated in Figure 3.13b. The inflection point, that is the value of $t_0 = t_{eff}$ for which $\mathrm{d}\Theta/\mathrm{d}t_0$ is at its greatest, is extracted from different system sizes. Henceforth, t_{eff} is plotted against L yielding Figure 3.13a and displaying power law dependence. $t_c \approx 0.61 \pm 0.02$ is then estimated by extrapolating t_{eff} to infinity, achieved by determining the exponent $b \approx 0.371 \pm 0.005$ which provides the best power law fit using equation 2.13, illustrated in Figure 3.13b. Finally, the critical exponent $\beta/\nu \approx 1.5 \pm 0.1$ is determined by the same approach as for t_c and b, and shown in Figure 3.14.

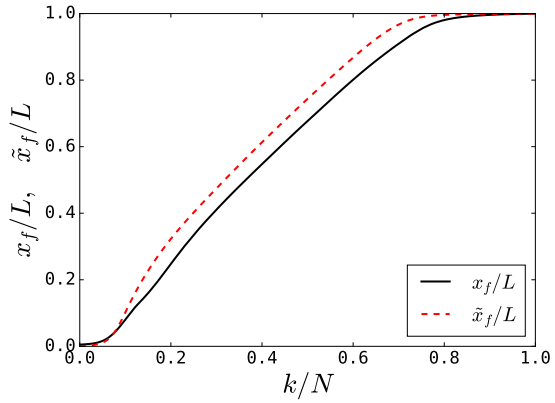

(a) Reduced and complete front positions, $\tilde{x}_f$ and x_f.

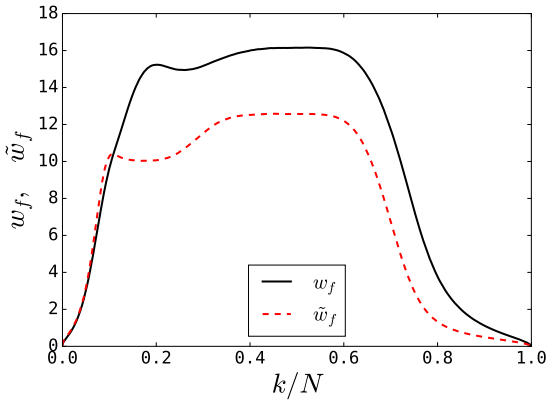

(b) Reduced and complete front widths, $\tilde{w}_f$ and w_f.

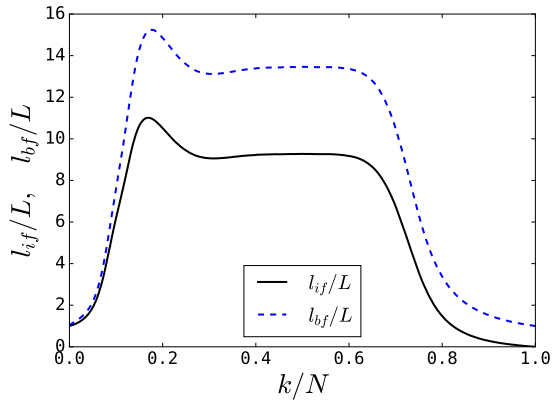

(c) Lengths of the intact and broken fronts, l_{if} and l_{bf}.

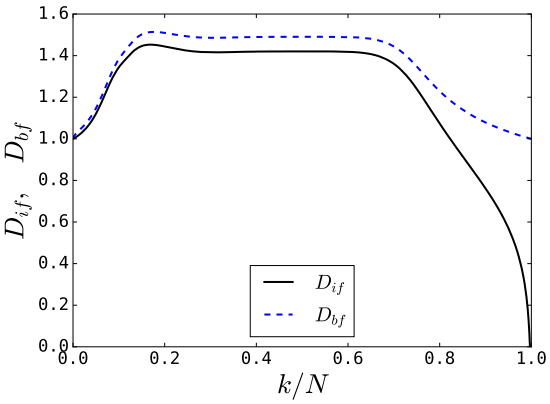

(d) Fractal dimensions of the intact and broken fronts, D_{if} and D_{bf}.

Figure 3.4: Resulting fracture front properties for an $N = 200^2$ system. The number of averaging samples for each data point is given by Table 3.1.

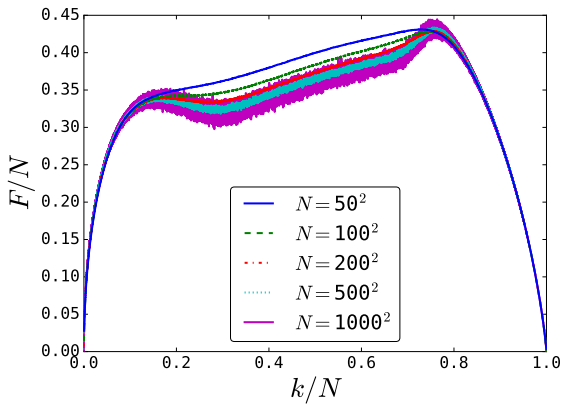

(a) Strain Curve.

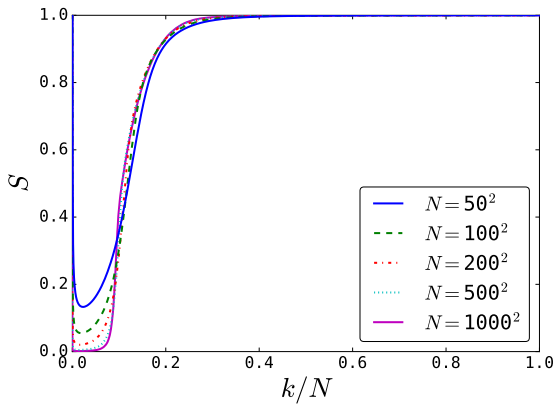

(b) Percolation Strength.

Figure 3.5: The strain curve and the cluster strength of the fiber bundle, as they develop in time for different lattice sizes. The number of averaging samples for each data point is given by Table 3.1.

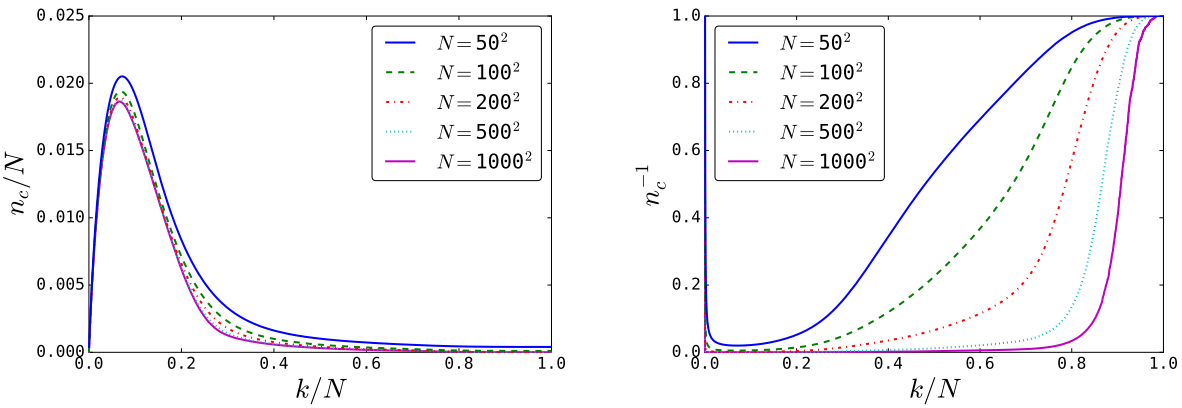

(a) Total number of clusters. **(b)** Inverted total number of clusters.

Figure 3.6: The total number of clusters and its inverse, as they develop in time for different lattice sizes. The number of averaging samples for each data point is given by Table 3.1.

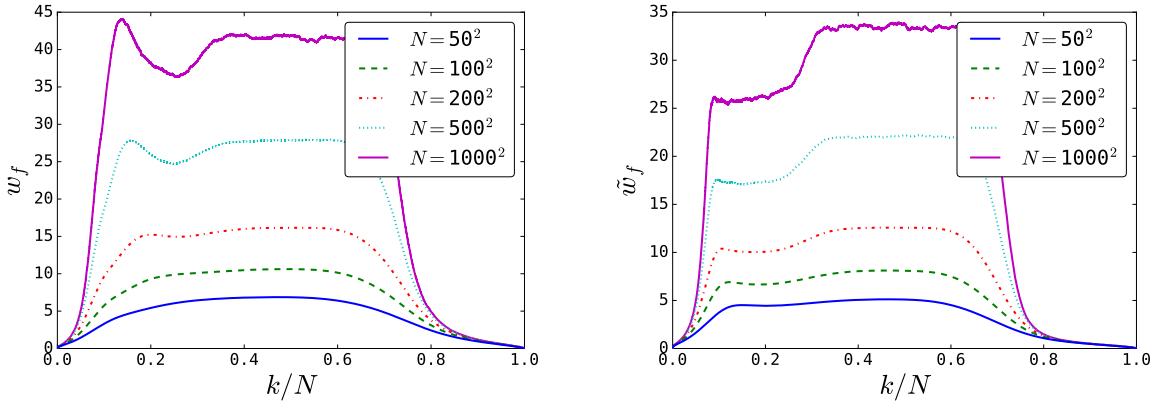

(a) Width of the complete front. **(b)** Width of the reduced front.

Figure 3.7: The widths of the fracture fronts as they develop in time, for different lattice sizes. The number of averaging samples for each data point is given by Table 3.1.

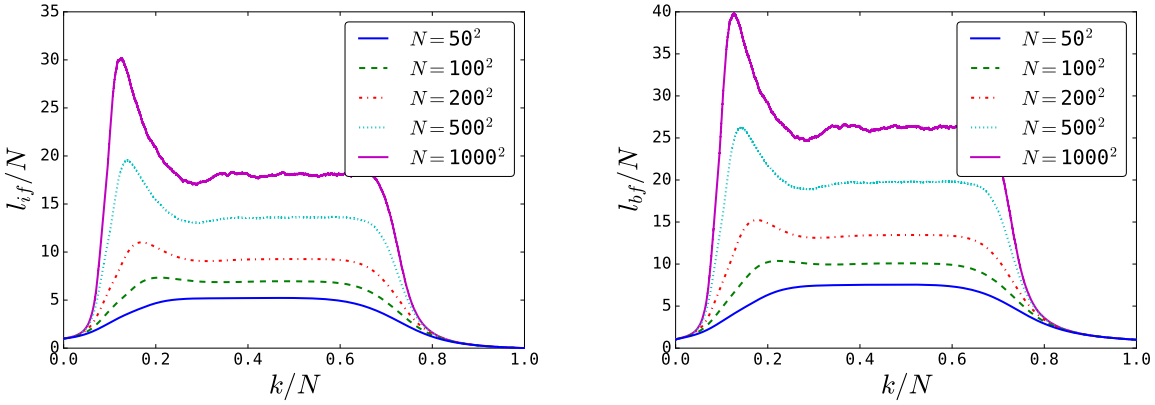

(a) Length of the intact front. **(b)** Length of the broken front.

Figure 3.8: The lengths of the fracture fronts as they develop in time for different lattice sizes. The number of averaging samples for each data point is given by Table 3.1.

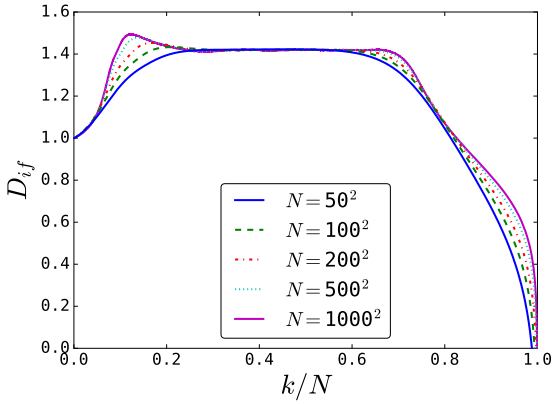

(a) Fractal dimension of intact front.

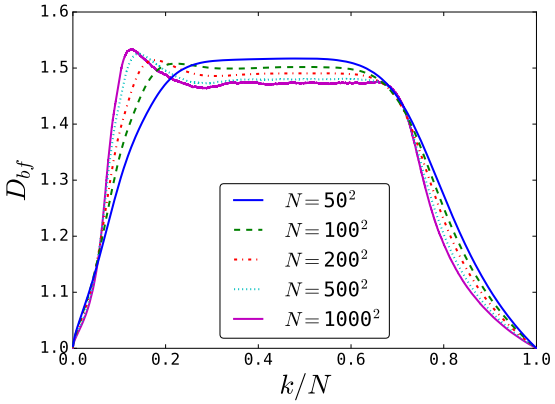

(b) Fractal dimension of broken front.

Figure 3.9: The fractal dimensions of the fronts as they develop in time for different lattice sizes. The number of averaging samples for each data point is given by Table 3.1.

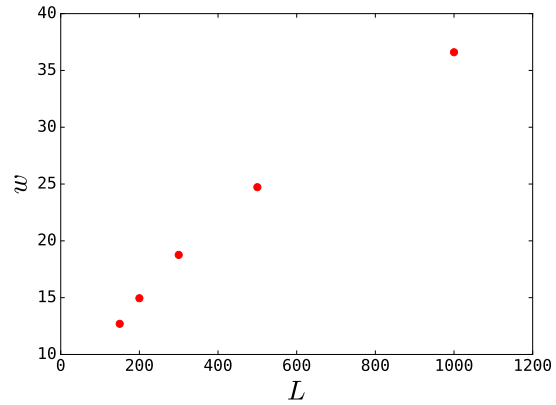

(a) Dependence the complete front's critical width on system size.

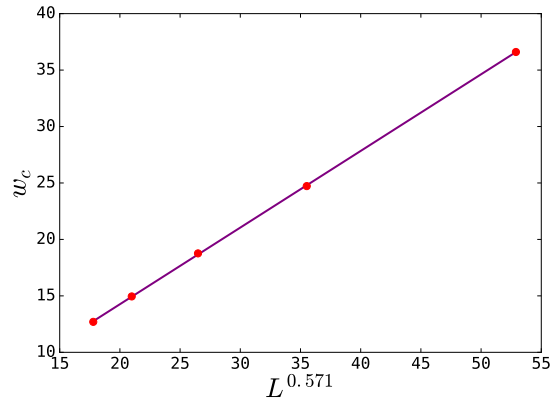

(b) Intercept $w_0 \approx 0.533$, slope $a \approx 0.700$ $\nu \approx 1.33$.

Figure 3.10: The critical width w_c is sampled from the local minimum occurring in the complete front's width, displayed in Figure 3.7a, and shown to obey a power law dependence on the lattice size L. The number of averaging samples for each data point is given by Table 3.1.

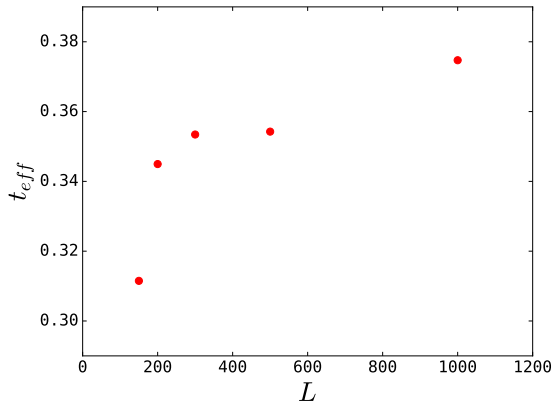

(a) Relation between t_{eff} and L.

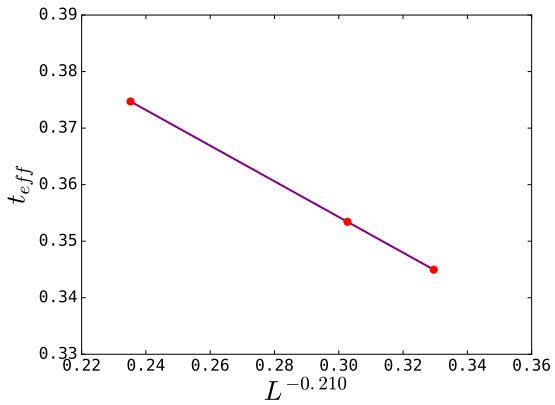

(b) Intercept $t_c \approx 0.45$, slope $a \approx -0.21$.

Figure 3.11: The effective, critical threshold t_{eff} is sampled from the local minimimum occuring in the CD width shown in Figure 3.7a, and shown to exhibit a power law dependence on the lattice size L. Only $L = \{300, 500, 1000\}$ has been utilized. The number of averaging samples for each data point is given by Table 3.1.

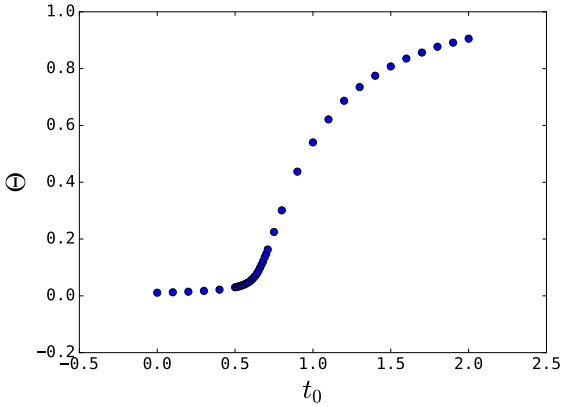

(a) $N = 30^2$.

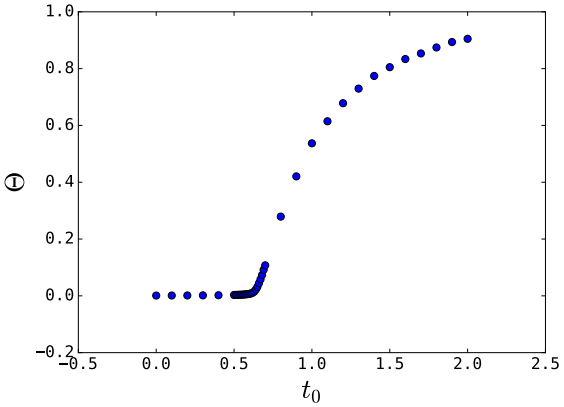

(b) $N = 100^2$.

Figure 3.12: The order parameter Θ from equation (2.12) is sampled for different values of t_0. The number of averaging samples for each data point is given by Table 3.1.

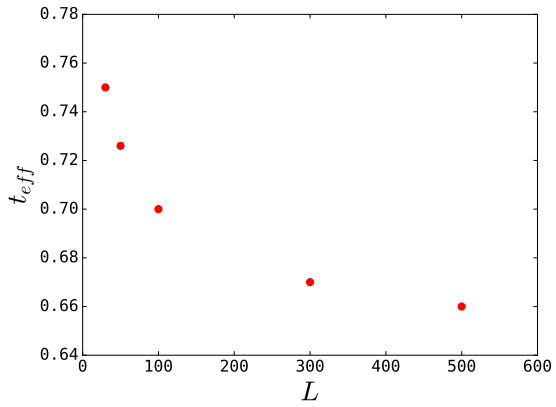

(a) Relation between t_{eff} and L.

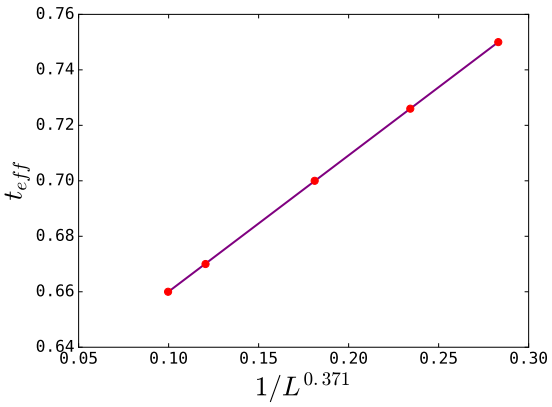

(b) Intercept $t_c \approx 0.611$, slope $a \approx 0.491$.

Figure 3.13: The effective critical threshold t_{eff} is compared against system size L to find the best power fit in order to extrapolate the fiber threshold to the thermodynamic limit and estimating t_c. The number of averaging samples for each data point is given by Table 3.1.

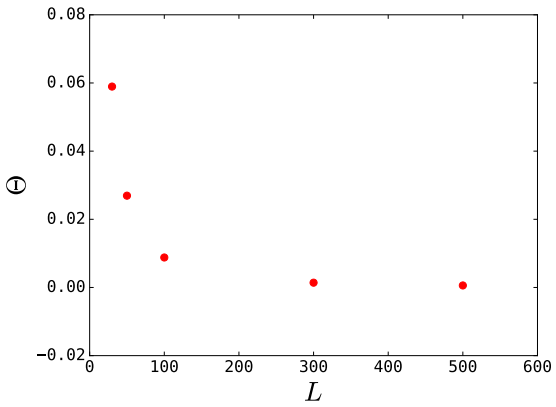

(a) The scaling relation between Θ and system size L, at $t_0 = 0.611$.

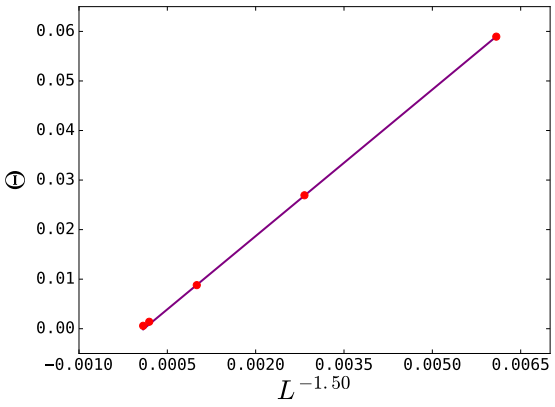

(b) Intercept $\Theta(0) \approx 0$, slope $a \approx 9.86$, exponent $-\beta/\nu \approx -1.50$.

Figure 3.14: The scaling relation between the order parameter Θ and system size L is studied to determine the exponent β/ν, providing the best power law fit of equation (2.14). The number of averaging samples for each data point is given by Table 3.1.

4 Discussion and Conclusion

4.1 Discussion

When comparing system and front properties for different system sizes in Figures 3.9, 3.8, 3.7, 3.5a, 3.6 it is clear that larger system sizes has greater fluctuations than smaller ones. This is confirmed by the overview of number of samples for each simulation given by Table 3.1. The number of samples could have been standardised by keeping the total number of fibers broken, $N \times$ (# of Samples), constant.

4.1.1 The Gradient System

Results confirm that the LLS FBM system with an imposed gradient in the cut-off t_0, in the threshold distribution, features the transition for which the damage spreading becomes localised (Figure 3.2), similar to the the system without a gradient (Figure 3.1). However, it should be emphasised that the imposed gradient changes the nature of the model. In general, increasing the cut-off in the exponential PDF will imply fiber thresholds to be numerically closer in the sense that the ratio $\min_{i\in\mathbb{F}}\{t_i\}/\max_{i\in\mathbb{F}}\{t_i\}$ decreases with growing t_0. A larger cut-off also increases the overall numerical values drawn from the PDF, making the fibers stronger. This latter effect won't influence the order of which fibers break in a system with constant t_0. However, for the gradient system it means that fibers on one side will be weaker compared to the other. This ultimately gives rise to the directed damage propagation, discussed in section 2.3. It also results in the early appearance of a spanning cluster in the system, which can easily be seen from the evolution of the percolation strength (Figure 3.3b and 3.5b), and the early appearance and decay of the peak of n_c (Figures 3.3c and 3.6a).

The occurrence of the spanning cluster can be considered as a percolation transition[1] and is also evident in other system properties. Consider for instance the front lengths of the intact (l_{if}) and broken (l_{bf}) fronts, which both display a global maximum near its appearance. This can be explained by how the initial damage spreading is similar

[1]Not to be confused with the localisation transition.

to that of the ELS FBM: Fibers break seemingly randomly[2], creating small islands of broken fibers. Then, the spanning cluster comes into existence as these islands connect and span over the entire system axis, perpendicular to the direction of the gradient. At this point in the process, the fracture front, or surface of the spanning cluster, has a very complicated and fractal geometry, resulting in the local maxima of the front lengths depicted in Figures 3.8a, 3.8b.

The fronts' lengths (l_{bf} and l_{bf}) drop again shortly after the appearance of the spanning cluster. This is due to how the breaking criteria from (1.6) will favor breaking fibers close to the spanning cluster. Surviving fibers in this region will be much more likely to neighbour a cluster, but also because the imposed gradient has also given these fibers statistically weaker thresholds. Thus, fibers positioned in the region close to the spanning cluster will be significantly relatively heavier loaded than fibers further away. Hence, fibers positioned inside the fractal geometry of the spanning cluster, or near the fracture front, break rapidly, reducing the fronts lengths and their fractal dimension (Figure 3.9).

The effect of the appearing spanning cluster is also visible on the fracture fronts' widths w_f and $\tilde{w}_f$, shown in Figures 3.4b and 3.7. By the same argument, the spanning cluster creates a complicated and fractal geometry, before it breaks it again, resulting in the global maximum of w_f. The reduced front however, is independent from the fractal geometry, since it consists only of the outer most fibers on each row. Hence, for large systems it stabilises and flattens out with the appearance of the spanning cluster. On the other hand, for small system sizes, the fracture front's surface is far less complicated, and the appearance of the spanning cluster pushes the innermost reduced front fibers out closer to the outer laying ones, resulting in a local minimum.

Also the strain curve (Figures 3.3a and 3.5a)is influenced by the appearance of the spanning cluster. Larger systems ($L > 100$) exhibit negative slopes in their strain curves at about $k/N \approx 0.2$, which indicates that fibers breaking within the complicated structure of the spanning are breaking in bursts. After the spanning cluster has devoured most of its fractal internals there is no where to go but to push east. This phase is indicated by the local stability in the strain curve seen in Figure 3.3a, indicating that the external force F needs to be increased in order to break the next fiber. At the same time, the front widths increases again moving out of their local minimum, and the damage spreading has

[2]The damage spreading of the ELS FBM is in reality not random at all [1].

effectively become localised. This is the critical transition point of localisation.

Beyond the localisation transition point, the fronts' widths increase again and settles at a steady value described by invasion percolation. As seen from Figure 3.9a, the fractal dimension of the external perimeter of the front steadily decreases with increasing system size, and is expected to converge towards $D_{if} = 4/3$ as a generally known result for invasion percolation dynamics [11]. The behaviour of the fractal dimension of the broken front (Figure 3.9b) however, is not completely understood by the author, as it settles as about $D_{bf} \approx 1.41$, independent of the system size.

When considering the calculation of the correlation length exponent and the estimation of t_c from gradient system, seen in figure 3.11, it is evident that the the cut-off t_0 has not been sampled at, or even close to, the effective critical cut-off t_{eff}, as seen from the poor power law fit. Moreover, the estimation of the correlation length exponent from Figure 3.10b, yields $\nu/(\nu+1) \approx 0.57$. This results suggests that, when compared to the exact exponent for invasion percolation $\nu_{ip} = 4/3$, that the localisation has already commenced.

It is probable that the transition does occur in the local minimum of w_f, or already at the occurance of the spanning cluster. However, it is likely to be a result of different effects unrelated to the existance of a critical cut-off threshold. Moreover, it may be a forced localisation due to the spatially distribution of thresholds in the system, as discussed above. That is, fibers neighbouring the spanning clusters have a much higher probability of breaking compared to fibers further away, not only for being relatively heavier loaded, but since they were assigned a lower threshold to begin with. By this argument, it would seem the gradient methods fails in locating the critical cut-off threshold t_c. Nevertheless, its result should be compared with those of the order parameter for consistency.

4.1.2 The Zero-Gradient System

The existence of a critical phase transition in the LLS FBM is well supported by the results provided by the order parameter's dependence on the cut-off threshold, illustrated in Figure 3.12. Evidently, the transition becomes sharper for increased system size, as is expected of a second order phase transition [13]. The effective critical cut-off t_{eff} provides a decent power law fit against the system size L (Figure 3.13), so that the effective critical threshold can extrapolated to the thermodynamic limit resulting in $t_c \approx 0.61$. This result coincides well with the findings of the first reported incident of the critical

phenomena [10]. With the estimation of t_c, it was possible to determine the critical exponent $\beta/\nu \approx 1.5 \pm 0.1$, (Figure 3.14). For comparison, invasion percolation has the corresponding exponent $(\beta/\nu)_{ip} = 0.11$, which indicated the LLS FBM to be characterised very differently from percolation systems.

One easily notices that the largest systems don't lay perfectly on the straight line of the power law fit in Figure 3.14, but indicates a slight curvature. This implies that the estimated critical cut-off is slightly off [12].

4.2 Conclusion

The results from the systems with and without an imposed spatial gradient in t_0 do not coincide. It is suggested that the onset of localisation in the gradient system occurs due to the early appearing spanning cluster in a region of relatively weaker fibers caused by the gradient. Evidently, this leads to a forced localisation unrelated to the existence of the critical cut-off parameter. Hence, the results obtained from investigating the order parameter are concluded valid over those obtained from the gradient system. Thus, by studying the order parameter's dependence on the cut-off parameter t_0, the critical cut-off threshold has been estimated to $t_c = 0.61 \pm 0.02$. Furthermore, the critical exponent $\beta/\nu = 1.5 \pm 0.1$ was determined by applying finite size scaling.

4.2.1 Directions for Future Research

Since the correlation length exponent of the transition ν could not be obtained within this work, it should be a natural topic for future research. It may be possible to prevent the occurrence of a spanning cluster to after the expected localisation transition by imposing the gradient such that $t_0 = 0$ in the center of the system and radially increasing outwards. However, such a gradient would also make the determination of the fluctuations (w_f) much more difficult to study. Also, forced localisation due to fibers being weaker at the center could also be expected in this system.

It would also be interesting to investigate why the fractal dimension of the broken front $D_{bf} \approx 1.41$, apparently is independent of the system's size, which is not the case for the intact front, slowly converging towards $D_{if} = 4/3$.

Finally, the precision of the numerical finding in this research should be improved

significantly, for by increasing the accuracy in t_c. The numerical procedures of this work are computationally comprehensive, and demands a huge amount of CPU hours for large system sizes. The amount of data points in Figure 3.12 showing the order parameter against t_0 should be increased significantly, along with the number of averaging samples for each data point. The number of samples should also be standardised such that $N \cdot$ (# of samples) is constant, yielding fluctuations of same order of magnitude for different system sizes.

References

[1] A. Hansen, P. C. Hemmer, and S. Pradhan, *The Fiber Bundle Model: Modelling Failure in Materials*, 1st ed. (Wiley-VCH, Weinheim, 2015).

[2] T. L. Anderson, *Fracture Mechanics: Fundamentals and Applications*, 3rd ed. (CRC Press, Boca Raton, 2005).

[3] A. A. Griffith, Phil. Trans. R. Soc. Lond. A **221**, 163 (1921).

[4] H. M. Westergaard, J. Appl. Mech. Trans. **6**, 49 (1939).

[5] G. R. Irwin, J. Appl. Mech. Trans. **24**, 361 (1957).

[6] K. S. Gjerden, *Role of Quenched Disorder in Fracture Front Propagation*, Ph.D. thesis, NTNU (2013).

[7] A. Stormo, *Brittle to Quasi-Brittle Transitions in the Soft Clamp Fiber Bundle Model*, Ph.D. thesis, NTNU (2013).

[8] F. T. Peirce, J. Text. Ind. **17**, 355 (1926).

[9] H. E. Daniels, Proc. R. Soc. A **183**, 405 (1945).

[10] J. Kjellstadli, *Investigating the Local Load Sharing Fibre Bundle Model in Higher Dimensions*, Master's thesis, NTNU (2015).

[11] D. Stauffer and A. Aharony, *Introduction to Percolation Theory*, 2nd ed. (Taylor & Francis, London, 1992).

[12] J. Brankov and D. Dantchev, *Theory of Critical Phenomena in Finite-Size Systems: Scaling and Quantum Effects*, 1st ed. (World Scientific, Singapore, 2000).

[13] H. E. Stanley, *Introduction to Phase Transitions and Critical Phenomena* (Oxford Univ. Press, Oxford, 1987).

[14] S. Sinha, J. T. Kjellstadli, and A. Hansen, Phys. Rev. E **92**, 20401 (2015).

[15] B. Sapoval, M. Rosso, and J. F. Gouyet, J. Phys. Lett. **46**, 149 (1985).

[16] R. M. Ziff and B. Sapoval, J. Phys. A **19**, 1169 (1986).

[17] A. Hansen and D. Stauffer, Phys. A **189**, 611 (1992).

[18] M. Rosso, J. F. Gouyet, and B. Sapoval, Phys. Rev. B **32**, 6053 (1985).

[19] K. S. Gjerden, A. Stormo, and A. Hansen, Phys. Rev. Lett. **111**, 135502 (2013).

[20] M. E. Fisher and M. E. Barber, Phys. Rev. Lett. **28**, 1516 (1972).

A Locating the Transition from System Properties

Considering the gradient system, the onset of localisation was determined to the local minimum of the width curve, by studying animations and still frames of the fiber breaking process in detail. By registering the time (number of broken fibers k) at which the localisation occurred, and investigating system properties for abnormal and critical behaviour at this time step, it was concluded that the localisation set in at complete front's width's local minimum. A set of still frames from the animations of the breaking process are presented below to support and illustrate this conclusion.

Figure A.1 illustrates the early stage of the process where the damage spreading sill behaves similar to the ELS FBM. The creation of the spanning cluster as islands of broken cluster merge together is shown in Figure A.2. Two illustrations are given for the transition point: At (Figure A.3) and after (Figure A.4) the transition. At the end, a still frame from the region of invasion percolation is show in Figure A.5, where the process damage spreading is fully localised.

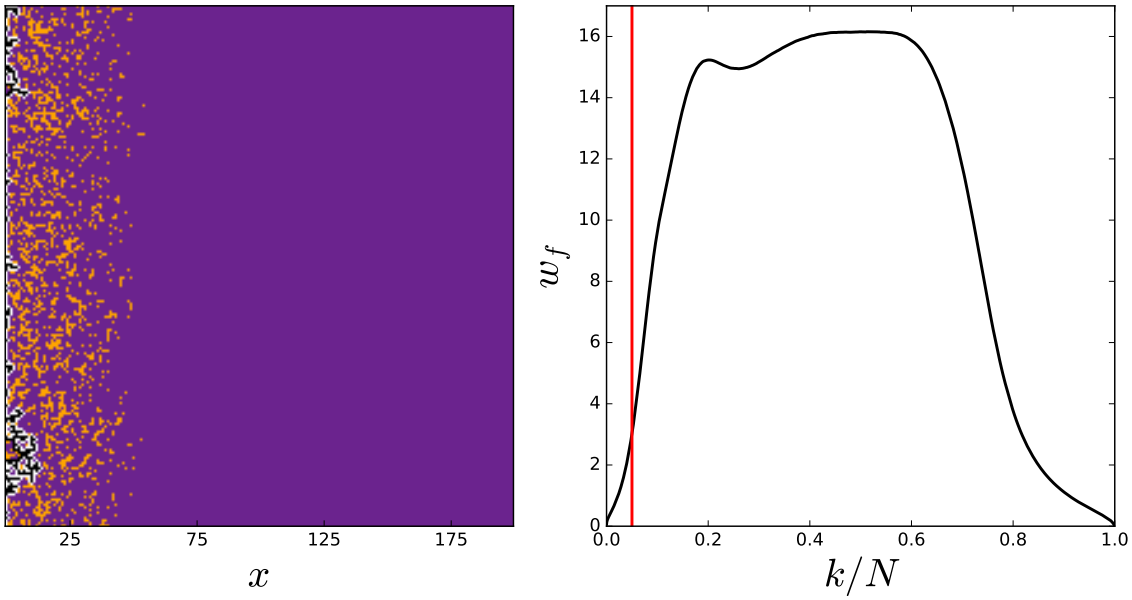

Figure A.1: A still picture from an animation of an $N = 200^2$ system at $k/N \approx 0.05$. The characteristics of the damage propagation at this stage are similar to that of the ELS FBM, but are gradually changing and about to become localised. The width curve w_f is made by averaging 800000 samples.

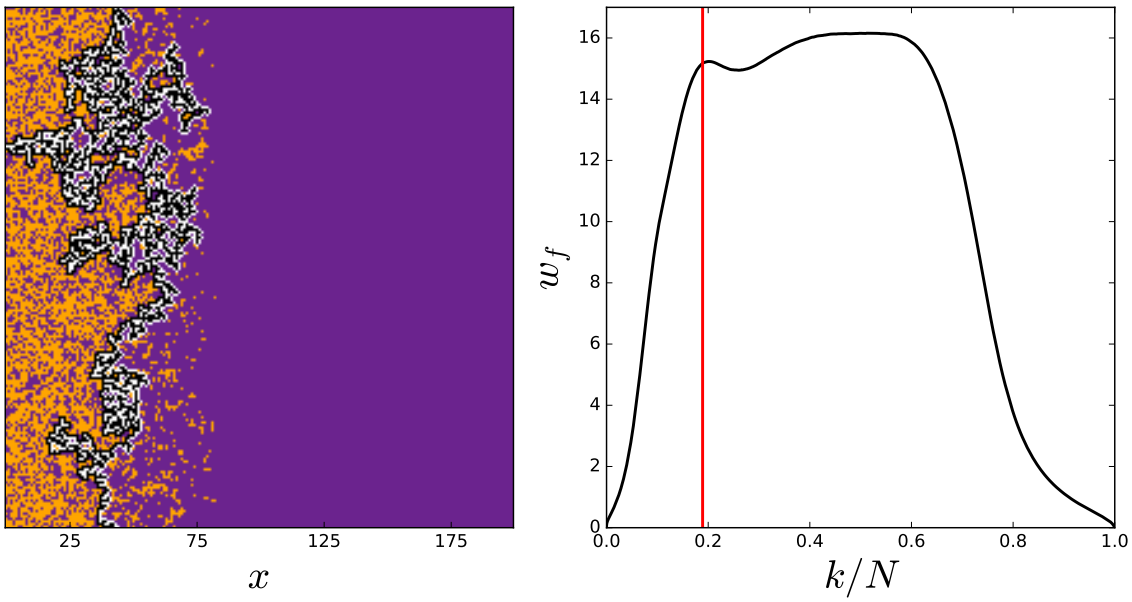

Figure A.2: A still picture from an animation of an $N = 200^2$ system at $k/N \approx 0.19$. The appearance of the spanning cluster happens just before the peak of the width curve w_f, which is made by averaging 800000 samples.

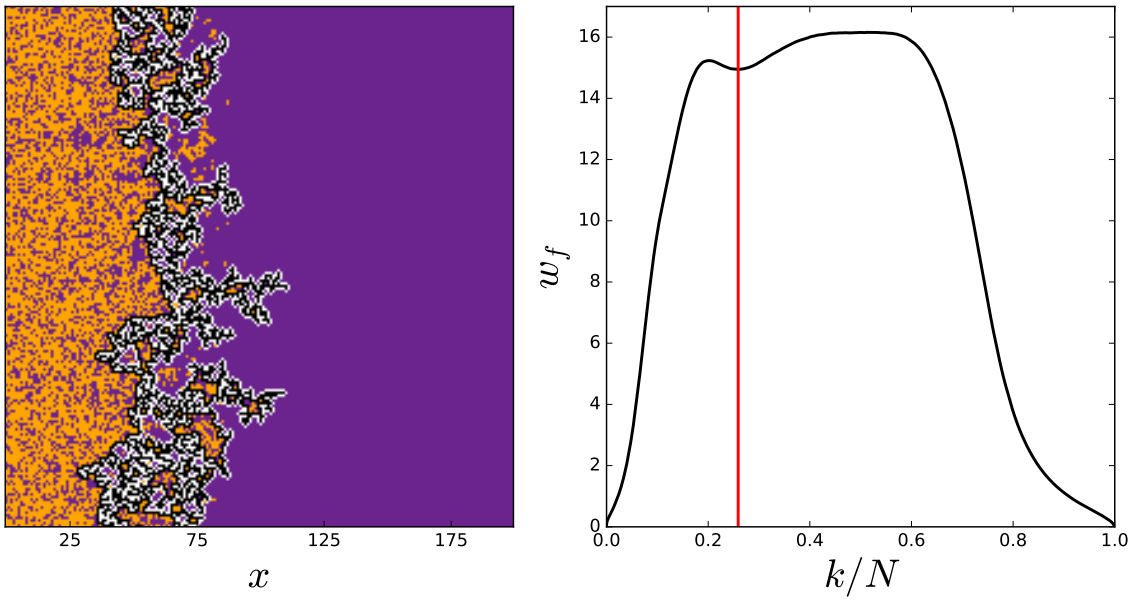

Figure A.3: A still picture from an animation of an $N = 200^2$ system at $k/N \approx 0.26$. The characteristics of the damage propagation is rapidly changing to become localised. The width curve w_f is made by averaging 800000 samples.

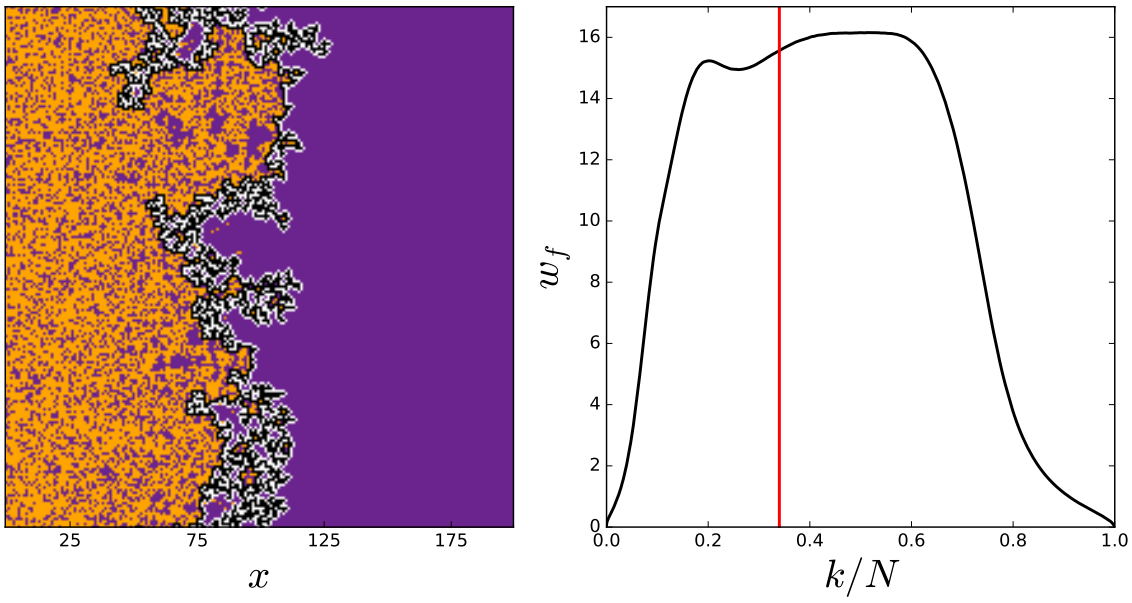

Figure A.4: A still picture from an animation of an $N = 200^2$ system at $k/N \approx 0.34$. The characteristics of the damage propagation have changed and become localised. The width curve w_f is made by averaging 800000 samples.

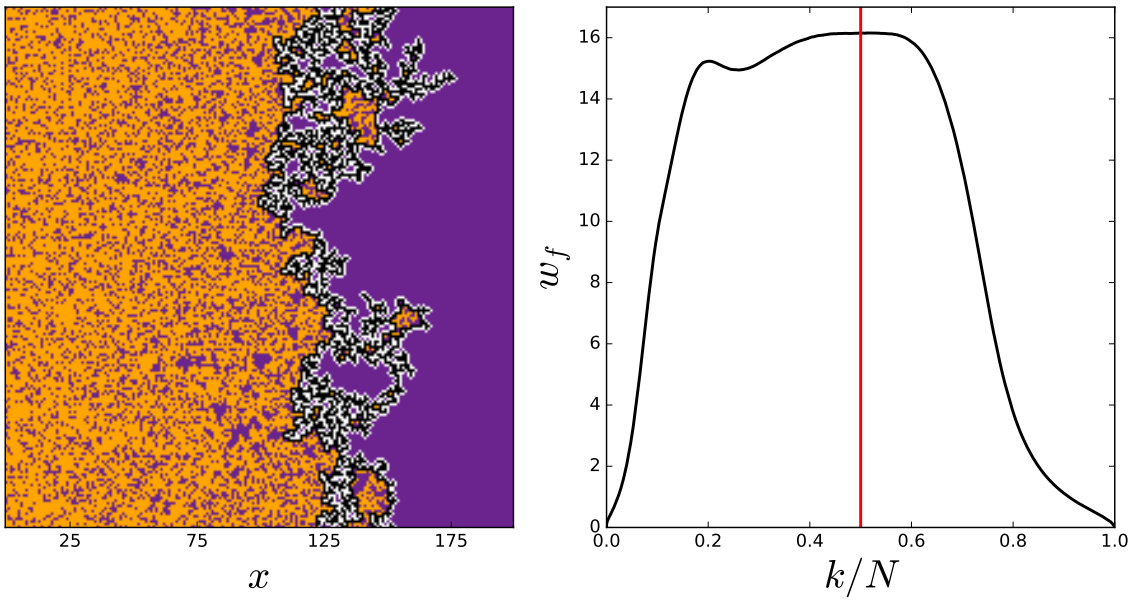

Figure A.5: A still picture from an animation of an $N = 200^2$ system at $k/N \approx 0.50$. The damage propagation is purely localised, dominated by invasion percolation. The width curve w_f is made by averaging 800000 samples.

B The Front Finder Algorithm

There exist multiple, different algorithms for searching and detecting edges in lattice systems. The method applied for this work is based on the simple concept of traversing the edge while always attempting to make a turn out of the object whose edge/surface is being traversed. Consider the system illustrated in Figure 2.1, which when including the ghost fibers of the zeroth column, can be treated as system with two infinite clusters: An infinite cluster of broken fibers to the left, and an infinite cluster of intact fibers to the right. Note that both of these contain finite clusters of the opposite kind within themselves, however, these will not affect the front-finding algorithm.

B.1 The Reduced Front

It is a trivial task to locate the reduced front: For each lattice row of the system, search from the east end to the west until a fiber belonging to the infinite broken cluster is found. These L fibers constitute the reduced front.

B.2 The Broken Front

Locating the nearest-neighbouring connected path of broken fibers can be achieved by the following set of instructions.

1. Choose an arbitrary row of the system lattice, and search from the east to the west side for the first appearance of a fiber which belongs to the infinite broken cluster.
2. Enumerate the four possible traversing directions, e.g. North [1], East [2], South [3], West [4]. These should be periodic in the sense that also [0] represents West, and [5] North.
3. Walk the edge going upwards by always turning right when possible.
4. Let c represent the current node/fiber being treated, d_{prev} be the direction from which was walked to reach c, and d_{next} be the direction in which the walker is about to leave c.

5. For the very first step one should impose $d_{prev} = 3 \vee 2$, and always traverse fibers of the broken infinite cluster only by,

   (a) Always attempting to turn right first: $d_{next} = d_{prev} + 1$

   (b) If turning right is not possible[1], then try the next best thing; Attempt $d_{next} = d_{prev} + 1 - q$, for $q \in [1, 4]$. One of these will always be possible.

   (c) Repeat until the entire surface/edge is mapped: That is, when the c is back as the very first node again ***and*** wants to leave it in the same direction as it did that very first time.

The reader should take special notice of the finishing criteria of the algorithm. It is not sufficient to finish after visiting the same fiber twice, as the fractal geometry of the front may contain long, thin arms forcing the traversing to return by the same path as it originally passed through, though not by the same directions.

Figure B.1 illustrates the traversing process, showing each of the four direction that can be taken. The white, filled circle represents the currently treated fiber c, while the vectors pointing to and from it represents the directions d_{prev} and d_{next} respectively. The filled, black circles represents direction which are checked, but not legal, next directions. These are intact fibers, not part of the infinite broken cluster, but are instead fibers which should be included in the intact front.

B.3 The Intact Front

Locating the front of intact fibers can provide a rather challenging problem if the method is expected to map it independently of the broken front, since its fibers can be connected by both nearest, and next-nearest neighbours. The most time efficient approach known to the author, is to incorporate the localisation of the intact front into the algorithm for locating the broken front. This is achieved simply by adding the fibers that are checked by the algorithm traversing the broken front, but not moved to science they are intact, and thus not part of the broken cluster. Essentially, this result in the following

Unchanged direction: The right-hand-side of c is added.

[1]This direction leads to a node which is *not* part of the infinite broken cluster.

Right-turn: No fibers are added.

Left-turn: Two fibers are added; (1) The neighbouring fiber (of c) in the same direction as d_{prev}, and (2) the neighbouring fiber of c in the *opposite* direction of d_{next}.

U-turn: Three fibers are added: *All* neighbouring fibers, except the one in direction d_{next}.

An illustrative example is given below in Figure B.1. Note that, given a complex, fractal geometry of the front, it is possible that some intact fibers may be added more than once. A record should thus be kept, of what fibers have already been included to avoid overestimating the length of the intact front.

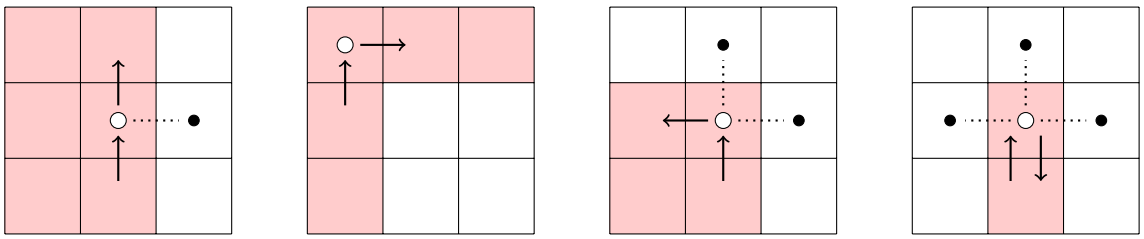

(a) No turn **(b)** R-turn **(c)** L-turn **(d)** U-turn

Figure B.1: Intact fibers are added to the intact front, by investigating what directions along the edge of the broken cluster is traversed. Colored (red) cells represents broken fibers of the infinite broken cluster. White cells represents intacts cells. The white circle indicates the currently treated fiber c of the broken front, and the connected black circles show its neighbouring intact fibers to be added to the intact front. Two vectors, pointing to and from fiber c, shows the previous direction d_{prev} and the next direction d_{next}, respectively, in accordance with traversing the broken front as detailed above.